CST04

The Second TSME International Conference on Mechanical Engineering
October 19 – 21, 2011, Krabi

Placement Angle Optimization in Physical Vapor Deposition Process

Temsiri Sapsaman[1,]*, Sasithon Bland[1], Karuna Tuchinda[2] and Surasak Surinphong[3]

[1] Dept. of Production Engineering, Faculty of Engineering, King Mongkut's University of Technology North Bangkok, 1518 Pibulsongkram Rd., Bangsue, Bangkok 10800 Thailand

[2] Dept. of Tool and Materials Engineering, Faculty of Engineering, King Mongkut's University of Technology Thonburi, 126 Pracha-utid Road, Bangmod, Toongkru, Bangkok 10140 Thailand

[3] NanoShield PVD Hard Coating
261/61 Mu 2, Panwithee Rd., Bangpriang, Bangbo, Samutprakarn 10560 Thailand

*Corresponding Author: E-mail: tsapsaman@gmail.com, Tel: (662) 9132500 ext 8208, Fax: (662) 5870029

Abstract

To significantly improve the lifespan of tools, manufacturers have widely used many surface coating processes. By creating high-energy beam of coating particles or plasma ions, Physical Vapor Deposition (PVD) process yields hard coating film due to high adhesion. However, the good property of coat can be achieved only with uniform coat thickness. Coating companies rely on their experience in performing the coating process to get the even coat, which may not be enough when dealing with unfamiliar or large work piece. To address the problem, a computer simulation is used to determine the optimal placement angle of the work piece that yields the most uniform coat. The 3D model of PVD process with multiaxial substrate rotation is developed to predict the thickness of coat with parameters found from experimental coating data. Parameters are found to be dependent of oven and setup, the number of rotation axes, and distance from self-rotation axis. The genetic algorithm is used to perform the optimization with the range and the standard deviation of coat thickness as objective functions. Simulation results show that when compared to a common-practice placement, optimal placement angles can improve the range and the standard deviation of coat thickness by up to 66.9% and 51.7%, respectively.

***Keywords**:* Physical Vapor Deposition (PVD) Simulation, Optimization, Genetic Algorithm.

1. Introduction

Widely used to improve the lifespan of tools in manufacturing industry, Physical Vapor Deposition or PVD process yields the hard coating film that can withstand corrosion and fatigue [1-5]. High quality coat comes from not only coating material but also the evenness of coat. Coat thickness should also be between 3 and 6 microns. Coating companies rely on their experiences to achieve uniform coat but that may not be enough when dealing with unfamiliar shapes and sizes of workpieces. Therefore, this work will try to use a computer simulation to predict the placement angle of the workpiece that gives uniform coat.

The computer simulation requires the calculation model of the PVD process. In 1994 Rother [6] proposed a 2-dimensional calculation model of the PVD process to predict the coat thickness. The predicted coat thickness obtained from the model has been compared to experimental data [7] and the model is also used to show the relevance between the arrangement of the jig fixture and the productivity [8]. The described model has parameters that are only dependent of the coating condition; however, these parameters are found to be dependent of the distance from the self-rotation axis as well. This work will use the 3-dimensional calculation model with parameters varied by the distance from the self-rotation axis. How to obtain these parameters will be discussed in details in the Parameter Calibration section.

In summary this paper presents a method of placement angle optimization in the PVD process using Genetic Algorithm (GA) algorithm, a 3-dimentional calculating model for the PVD process, and the parameter calibration. The paper also presents and discusses simulation results.

2. Placement Angle Optimization

To maximize the coating quality in terms of thickness range and even distribution, this study is interested in finding optimal placement angles for the PVD process of turbine blades, which is determined by using the genetic algorithm. Two objective functions, the range (= $T_p[\max] - T_p[\min]$ where T is coat thickness at points on the surface) and the standard deviation (SD) of the coat thickness, are used to evaluate each placement. While the SD is chosen as an objective function for the deviation reduction and evenness of thickness, the range is chosen for outlier reduction and the proper range of thickness. The simulation is performed using software for the multi-objective genetic algorithm by Dev *et. al.* [9].

2.1 PVD Thickness Calculation Model

Used to calculate the thickness of the coat on the surface, the 3-dimensional PVD calculation model presented here is followed the 2-dimensional model presented by Rother [6]. The coat thickness is calculated from the growth rate of particles depositing on the surface. Assumed to come from point sources, the strength of the particle vapor flux, j_v, from one source at a point on the substrate surface is described as

$$j_v = \frac{A}{r^2}(\cos\varphi)^n \qquad (1)$$

where A is the absolute value of the flux, r is the distance from the point to the source, φ is an angle between the source normal and the vector from the source to the point, as shown in Fig.1, and n is the distribution coefficient. The only positive value of $\cos\varphi$ is valid which implies that the point is located inside the oven, satisfying constraints.

Dependent of the film-forming particle flux, which is assumed to be equal to the particle vapor flux, the growth rate of the coat, $\dot{d}_c$, is described as

$$\dot{d}_c = \begin{cases} -j_v(H-S)\dfrac{m_c}{\rho_c}\cos\alpha, & \dfrac{\pi}{2} < \alpha < \pi \\ 0, & 0 < \alpha < \dfrac{\pi}{2} \end{cases} \quad (2)$$

where *H* is the sticking coefficient of the impinging particles, *S* is the sputtering coefficient, m_c is the average mass of the film-forming particle, ρ_c is the mass density of the condensed material, and α is an angle between the substrate surface normal and the vector from the source to the point, as shown in Fig.1. $\dot{d}_c$ becomes zero when α is between 0 and $\frac{\pi}{2}$, which means the substrate surface is not facing the source. Fig. 1 displays the flux parameters φ and α that are found from the vector from the source to a point on the surface, $\vec{r}$, the normal vector of the substrate surface at that point, $\vec{n}_{surface}$, and the source normal vector, $\vec{n}_{source}$.

The coat thickness at a point on the surface is the summation of the growth rate multiplied by time step, assuming that $\dot{d}_c = \frac{\Delta d_c}{\Delta t}$, where Δd_c is the change in coat thickness. The thickness calculation subroutine can be found in Fig. 2.

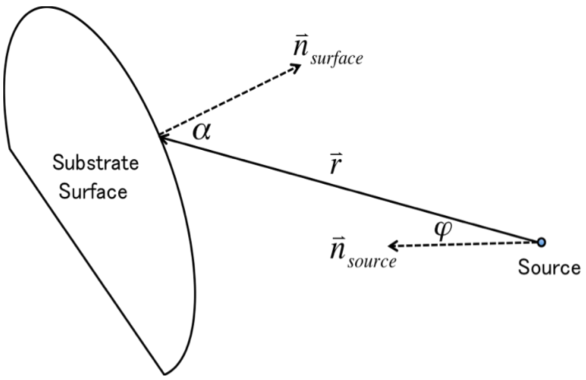

Fig. 1 Diagram of the flux parameters. $\vec{r}$ is the vector from a source to a point on the surface, $\vec{n}_{surface}$ is the normal vector of the surface at that point, and $\vec{n}_{source}$ is the source normal vector.

The distribution coefficient, *n*, the flux absolute value, *A*, the sticking and sputtering coefficients of the impinging particles, *H* and *S*, the average mass of the film-forming particle, m_c, and the mass density of the condensed material, ρ_c, are dependent of the coating process and conditions. These variables are experimentally obtained, which is explained in the next section.

initialize $T_p[j] = 0$
for $i = 0 : \Delta t$: last step
  find position vectors of interested points on substrate surface at current time
  for $j = 1$: last point
    $(\vec{r}_p)_j$ = position vector of point j^{th} on the substrate surface
    for $k = 1$: last source
      $(\vec{r}_s)_k$ = position vector of source k^{th}
      $\vec{r}_{j,k} = (\vec{r}_p)_j - (\vec{r}_s)_k$
      $r^2_{j,k} = \vec{r}_{j,k} \cdot \vec{r}_{j,k}$
      $\cos\varphi_{j,k} = \dfrac{\vec{r}_{j,k} \cdot (\vec{n}_{source})_k}{|\vec{r}_{j,k}|\,|(\vec{n}_{source})_k|}$
      $(j_v)_{j,k} = \dfrac{A}{r^2_{j,k}}(\cos\varphi_{j,k})^n$
      if $\frac{\pi}{2} < \alpha < \pi$
        $\cos\alpha_{j,k} = \dfrac{\vec{r}_{j,k} \cdot (\vec{n}_{surface})_k}{|\vec{r}_{j,k}|\,|(\vec{n}_{surface})_k|}$
        $(\dot{d}_c)_{j,k} = -(j_v)_{j,k}(H-S)\dfrac{m_c}{\rho_c}\cos\alpha_{j,k}$
        $T_p[j] = T_p[j] + (\dot{d}_c)_{j,k}\Delta t$
      end //if
    end //for
  end //for

Fig. 2 Coat thickness calculation subroutine.

3. System Modelling

Before the simulation can be done, all physical and PVD process parameters must be determined. While physical parameters can be directly measured, PVD process parameters are obtained from the actual PVD process and parameter calibration from the experimental coat thickness.

3.1 PVD Process and Physical Setup

The PVD process is performed in a cylindrical oven with twelve arcs in four-column arrangement. With 120 cm radius, the oven working area is 45 to 160 cm above the oven floor. The oven has one centered axis of rotation and six off-centered axes of rotation, which are connected by planetary gear and rotate three times faster than the centered axis. The workpiece can be fixed to both centered and off-centered axes at the oven ceiling. The centered workpiece has one axis of rotation and it is less constrained, while the off-centered workpiece has two axes of rotation and, being closer to the oven wall, it is more constrained. The off-centered workpiece rotates around itself and the center of the oven. The simulation will consider both placement locations. The angular speeds of the centered and off-centered rotation axes are presumed at 3 and 9 rpm, respectively.

With 10-minute warm-up, the PVD process takes about two hours or longer depended on the desired thickness. The experimental coat thickness is obtained from a two-hour process. Therefore, the simulation will calculate the coat thickness of the surface going through a two-hour process with the time step of 0.1 second.

3.2 Model Parameter Calibration

Due to the extreme nonlinearity of the deposition model, linearized curve fitting method is not suitable to obtain the calibration parameters. Instead, model parameters are obtained by calculating the coat thickness with the different values of parameters and comparing the calculated thickness to the experimental data. Parameters that give the coat thickness closest to the measured thickness are used in the angle placement optimization.

3.2.1 Experimental Data Collection

The coat thickness is measured from sample pieces coated under the real working condition. Two 24-piece rectangular sample sets are placed at the centered and the off-centered locations. Each set has sample pieces in fish-bone arrangement such that the tested surface of all pieces is on the same plane. Coat thickness is measured at four points on each sample piece, which are at 2, 4, 8, and 10 cm from the rotation axis. Calibration parameters are calculated for each distance from the rotation axis.

3.2.2 Calibrating Equation

By defining $C = A(H-S)\dfrac{m_c}{\rho_c}$, the coat thickness at point j^{th} on the substrate surface, $T_p[j]$, can be written in a closed form as

$$T_p[j] = \sum_{i=0}^{\#step}\left(\sum_{k=1}^{\#source}\left(\frac{-C}{r_{j,k}^2}(\cos\varphi_{j,k})^n \cos\alpha_{j,k}\,\Delta t\right)\right)_i,$$

$$\frac{\pi}{2} < \alpha < \pi \qquad (3)$$

When $\frac{\pi}{2} < \alpha < \pi$, $\cos\alpha_{j,k} < 0$; therefore, Eq. (3) can be rewritten as

$$T_p[j] = \sum_{i=0}^{\#step}\left(\sum_{k=1}^{\#source}\left(\frac{C}{r_{j,k}^2}(\cos\varphi_{j,k})^n\left|\cos\alpha_{j,k}\right|\Delta t\right)\right)_i \tag{4}$$

Eq. (4) has two unknown C and n. To find the values of C and n at each distance from center, several values of n are chosen and the following steps have been performed for each n. First, the value C_j is calculated for every data point in a set using

$$C_j = \frac{T_p[j]}{\Delta t\sum_{i=0}^{\#step}\left(\sum_{k=1}^{\#source}\left(\frac{(\cos\varphi_{j,k})^n\left|\cos\alpha_{j,k}\right|}{r_{j,k}^2}\right)\right)_i} \tag{6}$$

and C value is an average of all C_j. Second, the pair C and n are used to calculate the predicted thickness of every data point. Third, the root-mean-squared (RMS) error between the experimental and the predicted thickness is calculated for evaluation. The C and n that give the smallest RMS error is used for that distance.

3.2.3 Calibration Results

Eight sets of C and n are found for different coating conditions and distance from the self-rotation axis, as shown in Table. 1. In each case there are 24 data points. These parameters are used to predict the coat thickness, which is shown in comparison to the experimental data in Fig. 3. Parameters are found highly dependent of the distance from the self-rotation axis. Without the consideration of this dependency one set of parameters would be obtained for all distances and would have associated RMS errors equal to 0.194065 and 0.098548 for the centered and off-centered locations, respectively. This means with eighth sets of parameters the RMS errors in the thickness calculation are reduced by 27.18 – 53.16% at the centered location and 23.34 – 39.36% at the off-centered location.

4. Simulation Results

The GA simulation is done for the two-hour PVD process, in which the turbine blade is placed at centered and off-centered locations with the corresponding radial constraint of 55 and 22 cm, respectively. At each location two runs are performed. The 600/150 run has the number of the population equal to 600 and the number of generations equal to 150 with the random seed of 0.7. The 1800/50 run has the number of the population increased to 1800 and the number of generations reduced to 50 with the random seed of 0.5. In all runs results at each generation are compared to that of the zero-angle placement, in which the blade is placed straight down.

Table. 1 Model parameters obtained for different placement locations and distance from the self-rotation axis along with their associated RMS errors.

	Distance from rotation axis	n	C (x10^{-5})	RMS Error
Centered Location	2 cm	0.0001	2.28416	0.090906
	4 cm	0.0001	2.31249	0.091095
	8 cm	0.00001	3.10903	0.141319
	10 cm	0.0001	3.18449	0.128469
Off-centered Location	2 cm	5.6875	6.33093	0.075549
	4 cm	0.0001	2.15325	0.064133
	8 cm	0.0001	2.50428	0.065218
	10 cm	0.0001	2.52188	0.059761

Figs. 4-7 present the values of range versus SD of all population in different generations from 600/150 and 1800/50 (Figs. 6-7) runs for centered (Figs. 4 and 6) and off-centered (Figs. 5 and 7) locations. The red circles in all plots present the range and SD from the straight-down placement. Results from the 600/150 runs (in Figs. 4-5) show that solutions start to converge at the 20th generation. Therefore, the simulation can be run at the smaller number of generations. Results from 1800/50 runs are similar to those of the 600/150 runs, covering the same areas on plotting axes. Final results from both runs are virtually identical.

When the two placement locations are compared, the characteristics of results show the nature of locations. The less-constrained centered location gives the population with the larger variation of range and SD than that of the off-centered location at the first generation. Placing the turbine blade at the centered location yields better results than placing it at the off-centered location as the last-generation population of the

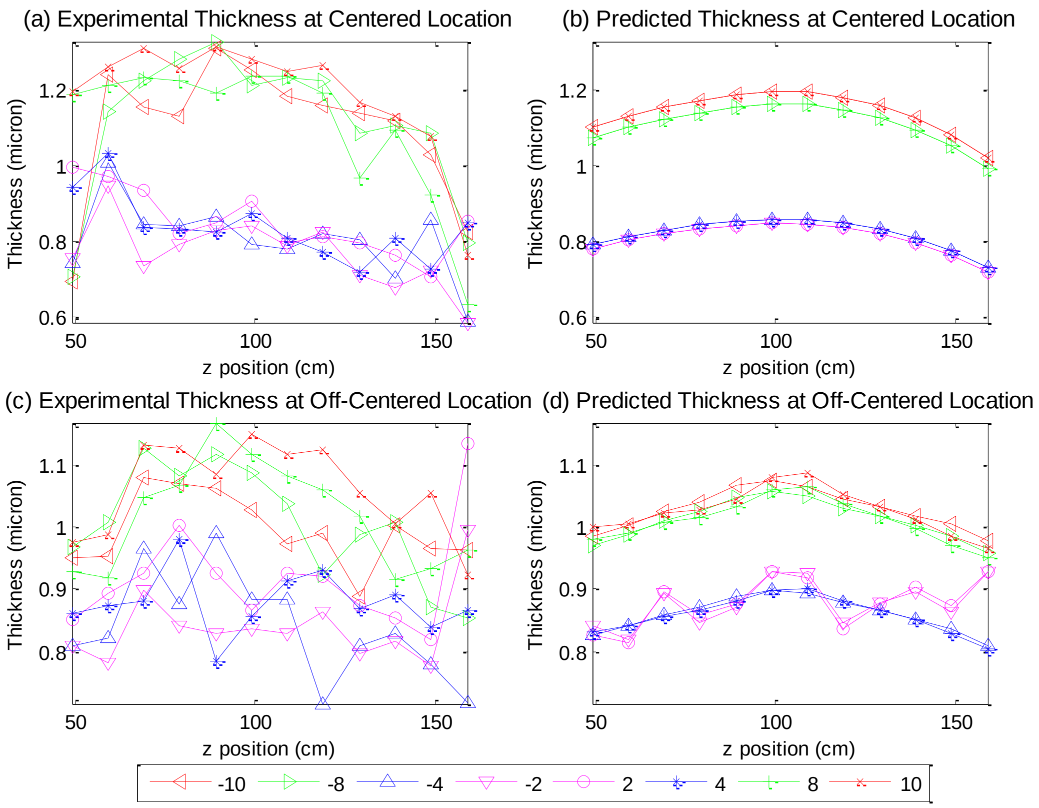

Fig. 3 Comparison between experimental coat thickness from samples placed at (a) centered and (c) off-centered locations and predicted coat thickness for samples placed at (b) centered and (d) off-centered locations.

centered location has range and SD lower than those of the last-generation population of off-centered location. These imply that the centered location give more even coat than the off-centered location.

At the centered location the GA simulation finds placement solutions that improve range by 60.4-66.9% and SD by 37.7-51.7%. At the off-centered location, obtained placement solutions can improve range by 18.2-31.9% and SD by 16.2-18.5%. These results show that the less-constrained centered location allows more improvement than the off-centered location. The absolute values of range and SD and their improvement suggest that the turbine blade should be placed at the centered location.

5. Discussion

The GA simulation gives placement solutions yielding better results than the straight-down placement. However, in choosing the best solution from these placement solutions other considerations must be taken into account. Since range and SD do not have a linear relationship, the method of solution ranking must be used to determine the best solution. Another quantity to be considered is the absolute value of thickness. Although the evenness of the coat is important, the thickness at all points should be around the 3-6 microns. The best solution should also have angle values that can be physically implemented easily and not sensitive to the placement error.

In conclusion, the proposed method offers a systematic way for workpiece placement. The next phase of this work is to determine the best placement solution. This placement will be used to perform the PVD coating on the turbine blade mock-up to validate the thickness calculation model and reassure that the actual range, SD, and absolute thickness values are acceptable.

6. Acknowledgement

This work is financially supported by Electricity Generating Authority of Thailand (EGAT), which is greatly appreciated. In addition, authors would like to express our gratitude toward NanoShield PVD Hard Coating for the experimental data.

7. References

[1] S. Korablov, M. A. M. Ibrahim, and M. Yoshimura (2005). Hydrothermal corrosion of TiAlN and CrN PVD films on stainless steel, *Corrosion Science*, vol. 47, 2005, pp.1839–1854.

[2] V. K. W. Grips, H. C. Barshilia, V. E. Selvi, Kalavati and K. S. Rajam (2006). Electrochemical behavior of single layer CrN, TiN, TiAlN coatings and nanolayered TiAlN/CrN multilayer coatings prepared by reactive direct current magnetron sputtering, *Thin Solid Films*, vol. 514(1-2), 30 August 2006, pp. 204–211.

[3] K. Fujita (2005). Research and development of oxidation, wear and corrosion resistant

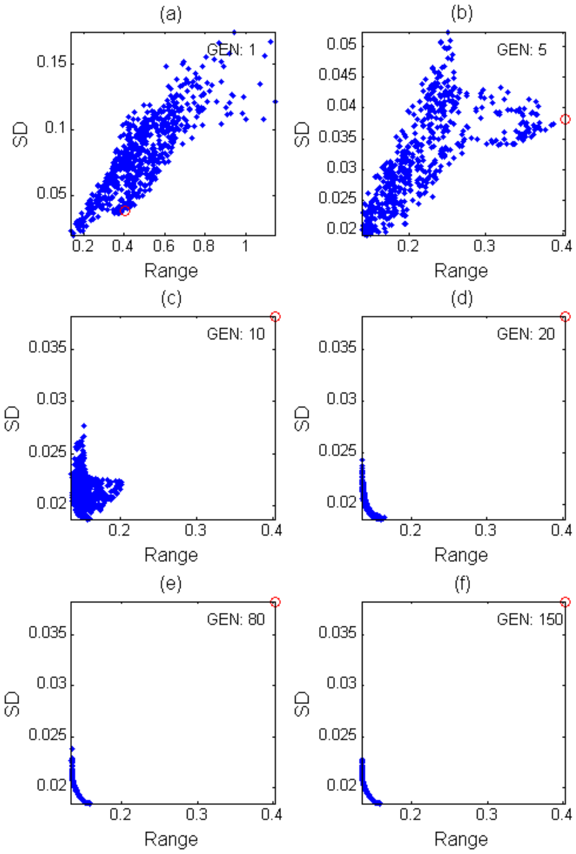

Fig. 4 GA results for the 600/150 run at the centered location show range and SD of all population in the (a) 1st, (b) 5th, (c) 10th, (d) 20th, (e) 80th, and (f) 150th generation.

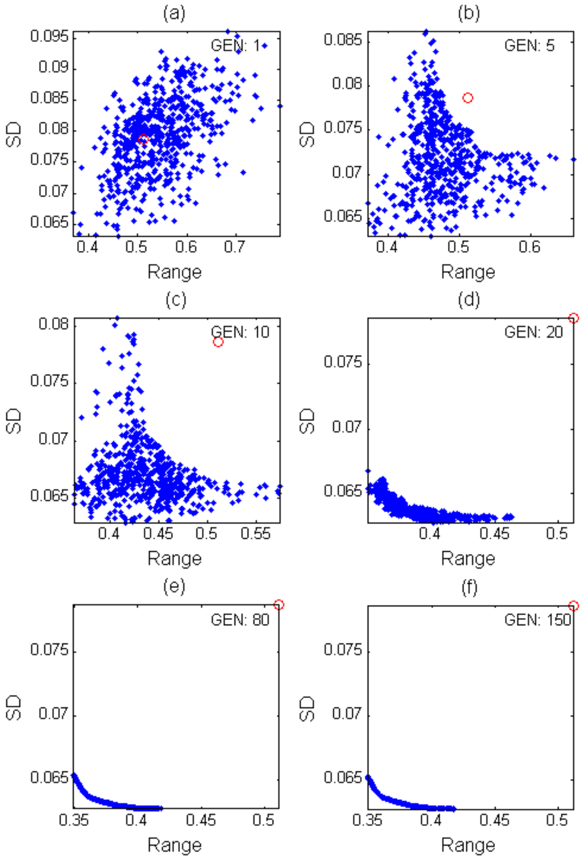

Fig. 5 GA results for the 600/150 run at the off-centered location show range and SD of all population in the (a) 1st, (b) 5th, (c) 10th, (d) 20th, (e) 80th, and (f) 150th generation.

materials at high temperature by surface modification using ion processing, *Surface &Coatings Technology,*vol.196, 2005, pp.139–144.

[4] Y. C. Chim, X. Z. Ding, X. T. Zeng, and S. Zhang (2009). Oxidation resistance of TiN, CrN, TiAlN and CrAlN coatings deposited by lateral rotating cathode arc, *Thin Solid Films*, vol. 517, 2009, pp. 4845–4849.

[5] J. L. Mo, and M. H. Zhu (2009). Tribological oxidation behavior of PVD hard coatings, *Tribology International*, vol. 42(11-12), December 2009, pp. 1758-1764.

[6] B. Rother (1994). On the possibility of physical vapour deposition process design by coordinated substrate rotation modes, *Surface and Coatings Technology,* vol. 64(3), 1994, pp. 155-159.

[7] B. Rother, H. A. Jehn, and H. M. Gabriel (1996). Multilayer hard coatings by coordinated substrate rotation modes in industrial PVD deposition systems, *Surface and Coatings Technology,* vol. 86-87, 1996, pp. 207-211.

[8] B. Rother, G. Ebersbach, and H. M. Gabriel (1999). Substrate-rotation systems and productivity of industrial PVD processes, *Surface and Coatings Technology,* vol. 116-119, 1999, pp. 694-698.

[9] K. Deb, A. Pratap, S. Agarwal, and T. Meyarivan (2002). A Fast and Elitist

Multiobjective Genetic Algorithm: NSGA-II, *IEEE Transaction on Evolutionary Computation*, vol. 6(2), 2002, pp. 182-197.

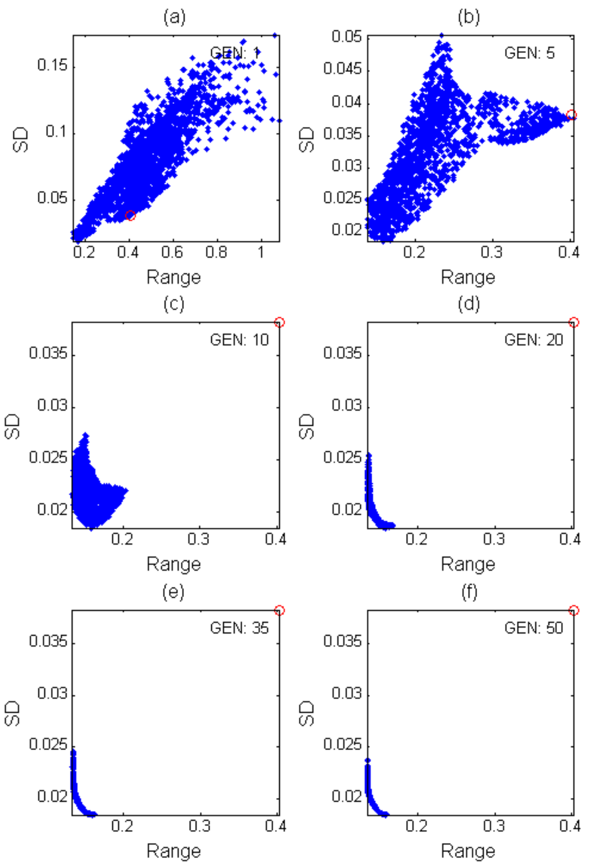

Fig. 6 GA results for the 1800/50 run at the centered location show range and SD of all population in the (a) 1st, (b) 5th, (c) 10th, (d) 20th, (e) 35th, and (f) 50th generation.

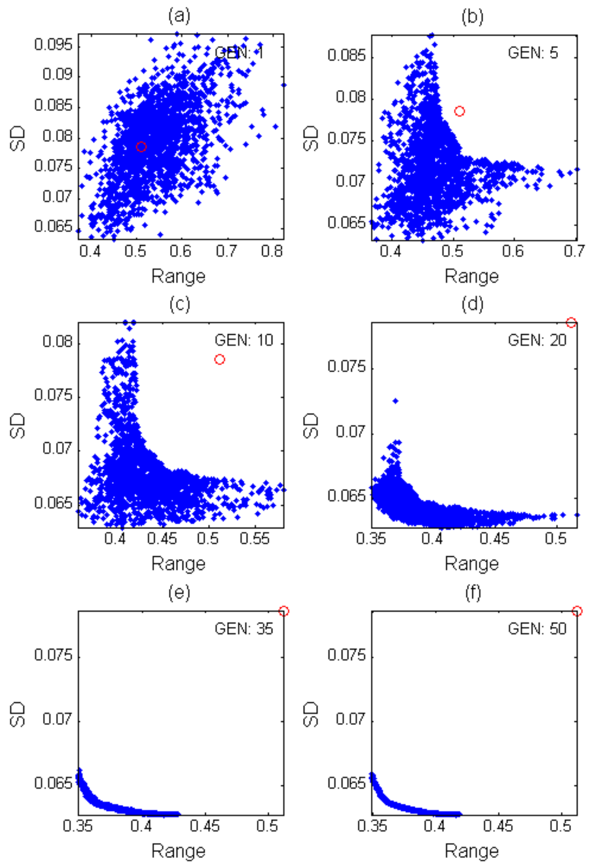

Fig. 7 GA results for the 1800/50 run at the off-centered location show range and SD of all population in the (a) 1st, (b) 5th, (c) 10th, (d) 20th, (e) 35th, and (f) 50th generation.